

Elimination of PPG Signal Disturbances through Variational Mode Decomposition and Hilbert Transform

Thanh Trung Thai, Thanh Tung Luu*, Khanh Duy Phan

Department of Construction Machinery and Handling Equipment, Faculty of Mechanical Engineering, Ho Chi Minh City University of Technology (HCMUT), Vietnam

Correspondence

Thanh Tung Luu, Department of Construction Machinery and Handling Equipment, Faculty of Mechanical Engineering, Ho Chi Minh City University of Technology (HCMUT), Vietnam

Email: luuthanhtung2002@gmail.com

History

- Received: 03-3-2024
- Accepted: 04-7-2024
- Published Online: 30-9-2024

DOI :

<https://doi.org/10.32508/stdjet.v7i2.1346>



Copyright

© VNUHCM Press. This is an open-access article distributed under the terms of the Creative Commons Attribution 4.0 International license.



ABSTRACT

The PPG signal presents considerable promise as a non-invasive technique across various applications. However, effectively utilizing this signal in real-world scenarios demands meticulous handling to identify and rectify disturbances within the photo-plethysmography (PPG) signal. Among the methodologies explored, integrating time-frequency spectra with a hybrid deep learning model, such as convolutional – long short term memory neural network model (CNN-LSTM), has emerged as a promising approach. Yet, prevalent methods often rely on Fourier-based algorithms for extracting time-frequency spectra, which are prone to energy leakage issues. To surmount this limitation, decomposition methods like Variational Mode Decomposition (VMD) coupled with the Hilbert transform offer a compelling solution. In this study, we propose a novel algorithm leveraging VMD and Hilbert transform to extract time-frequency spectra as features for a convolutional neural network model (CNN). Unlike studies employing Fourier-based time-frequency spectra and the hybrid CNN-LSTM model, this approach adopts a simpler architecture, relying solely on a CNN model. This simplicity owes to the efficacy of VMD and Hilbert transform in feature extraction, streamlining the computational process without sacrificing accuracy. Remarkably, our method yields high-performance outcomes, achieving accuracy, precision, and recall of 0.91, 0.95, 0.88, respectively on the MIMICIII dataset. These results underscore the robustness and effectiveness of our proposed methodology, offering promising avenues for enhanced utilization of the PPG signal in diverse biomedical applications. By amalgamating advanced signal processing techniques with deep learning models, our approach contributes to the advancement of non-invasive biomedical signal processing, potentially healthcare monitoring and diagnosis.

Key words: photo-plethysmography, photo-plethysmography signal processing

INTRODUCTION

Photoplethysmography (PPG) is a non-invasive technique that is used to detect blood volume variations through an infrared light sensor placed on the surface of the skin^{1,2}. Correct identification of the PPG waveform and its main features is essential in order to extract several biomarkers, such as heart rate, blood pressure, cardiac output, and blood oxygen saturation, when the red and infrared light are used simultaneously^{1,3}. However, the practical application of PPG encounters difficulties as this signal is easily influenced by users' movements. Consequently, the identification and removal of disturbed PPG segments within the overall signal are crucial.

The initial and most basic technique for assessing the PPG signal involves the Signal Quality Index (SQI). This approach partitions the PPG signal into multiple segments, subsequently computing the SQI for each segment. A segment is deemed to be of high quality if its SQI value exceeds a predefined threshold⁴. The foundation of this method relies on the observation that PPG signal waveforms undergo periodic

changes, consequently, the SQI associated with these signals is expected to exhibit a specific distribution pattern⁵. Figure 1 indicates the disparity in kurtosis and skewness distribution between quality and poor-quality PPG signal. However, a drawback of the SQI method lies in the multitude of proposed quality indices. Despite Elgendi's survey,⁶ favoring "skewness" as the optimal index, establishing a universal threshold for these indices remains challenging.

The application of deep learning models can address the limitations of the SQI method by employing a deep model to learn the distinguishing features of high-quality PPG signals. Li et al.⁷ utilized the Dynamic Time Warping (DWT) technique and a multi-layer perceptron model to evaluate PPG signal. This method was proposed to address physiological blood flow variations, leading to changes in the morphology of PPG signals. Esgalhado et al.⁸ conducted a survey on deep learning models to eliminate poor-quality PPG signal segments. The study compared Long Short-Term Memory (LSTM), Bidirectional LSTM, and Convolutional Neural Network (CNN) models.

Cite this article : Thai T T, Luu T T, Phan K D. **Elimination of PPG Signal Disturbances through Variational Mode Decomposition and Hilbert Transform.** *Sci. Tech. Dev. J. – Engineering and Technology* 2025; 7(2):2258-2266.

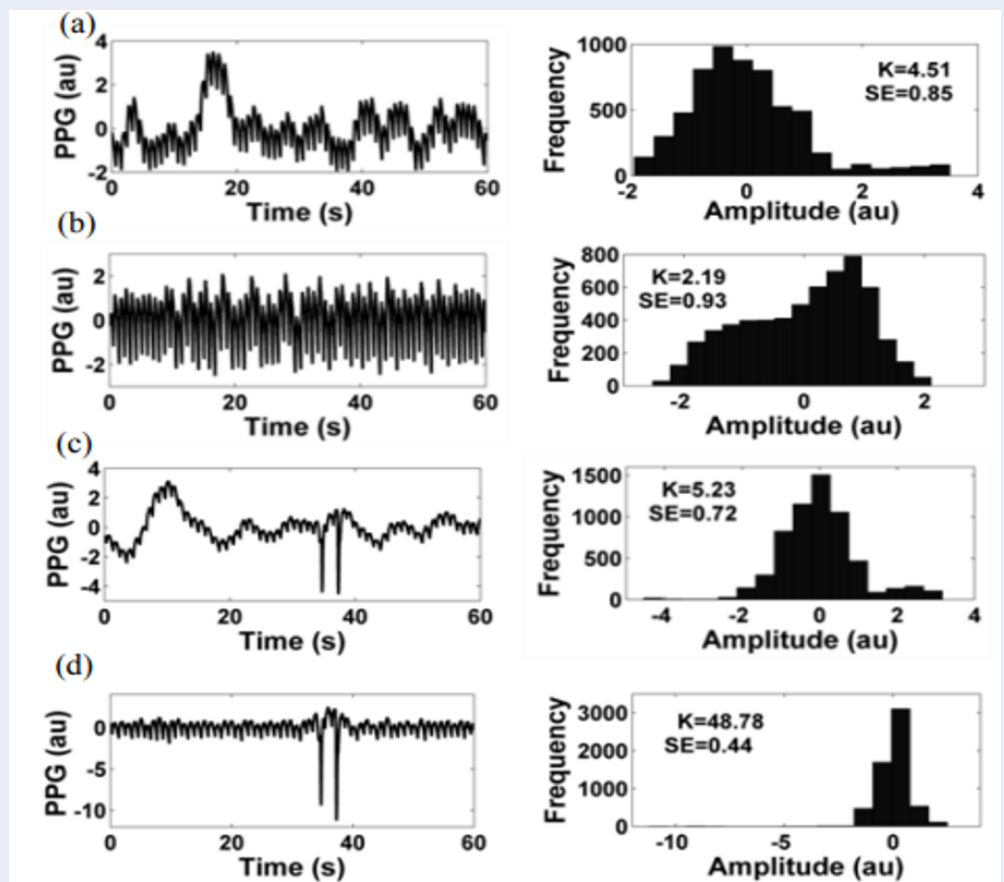


Figure 1: Sample clean (a-b) and corrupted (c-d) ear-PPG segments applied with linear (a, c) and 32nd order polynomial detrends (b, d) are shown along with their respective histograms and calculated kurtosis (K) and Shannon entropy (SE) values. The higher-order polynomial detrending is critical to enhance the specificity in the presence of physiological baseline drift (a) and the sensitivity in the presence of artifacts (c),⁴.

Besides, they also considered about the input data for the model. The research findings indicated that the CNN-LSTM algorithm, with Synchrosqueezed Fourier Transform (SSFT) input, demonstrated the highest performance with accuracy, 0.894. To explain the effectiveness of their approach, the authors explained that applying a time-frequency transform to the signals before classification provided the model with an expanded feature set. This extended dataset also facilitates signal projection from the time to the time-frequency domain, where non-stationary components may be better represented. Similar studies utilizing comparable deep learning models can be found in⁹.

It can be seen that deep learning model with a time-frequency input is a good choice for detecting and removing non-quality part in PPG signal. However, Fourier based method like SSFT representations has drawbacks regarding “energy leakage”¹⁰. This is a

phenomenon where energy regions of the signal have low concentration density, leading to some errors in CNN model processing. This drawback can be overcome by a method using VMD and Hilbert transform to create combined time-frequency spectra with CNN networks to identify and eliminate PPG signal segments affected by user motion.

MATERIALS-METHODS

Generating time – frequency spectrum

Instead of employing SSFT as in prior research, this study utilized VMD to decompose the raw PPG signal into sub-signals known as Intrinsic Mode Functions (IMFs). Subsequently, dominant IMFs were selected to generate a time-frequency spectrum by using the Hilbert transform. VMD, introduced by Dragomiretskiyi et al.¹¹, decomposes a signal into signals, called

Intrinsic Mode Functions (IMFs) in form:

$$IMF(t) = A(t) \cdot \cos(\phi(t)) \tag{1}$$

where A(t) is the amplitude over time, $\phi(t)$ is the frequency over time.

VMD determine the central frequency band of each IMF and proceed to analyze the original signal into IMFs with frequency domains around the central frequency. By pre-defining the number k of IMFs that the signal can have, computing the IMF channels is performed by a recursive loop:

In the (n+1)th iteration, the kth IMF is computed as follows:

$$U_k^{n+1}(f) = \frac{x(f) \sum_{i < k} U_i^{n+1}(f) - \sum_{i > k} U_i^n(f) + \frac{\wedge^n}{2}(f)}{1 + 2\alpha \{2\pi(f - f_k^n)\}^2} \tag{2}$$

$U_k^{n+1}(f)$ is the Fourier transform of the kth IMF in the (n+1)th iteration.

Along with that, the central frequency and the Lagrange multiplier are also updated.

kth central frequency, f_k^{n+1} :

$$f_k^{n+1} = \frac{\int_0^\infty |U_k^{n+1}(f)|^2 f df}{\int_0^\infty |U_k^{n+1}(f)|^2 df} \approx \frac{\sum f |U_k^{n+1}(f)|^2}{\sum |U_k^{n+1}(f)|^2} \tag{3}$$

Lagrange multiplier:

$$\wedge^{n+1}(f) = \wedge^n(f) + \tau (X(f) - \sum_k U_k^{n+1}(f))$$

where τ is the update rate of the coefficient Larrange.

When the algorithm satisfies the following condition, the loop stops:

$$\begin{cases} \sum_k \frac{\|u_k^{n+1}(t) - u_k^n(t)\|_2^2}{\|u_k^n(t)\|_2^2} < \epsilon_r \\ \sum_k \|u_k^{n+1}(t) - u_k^n(t)\|_2 < \epsilon_a \end{cases} \tag{4}$$

In this work, the PPG signal was decomposed into IMF channels through the VMD, with the algorithm's parameters as follows:

Number of IMF channels

The number of IMF channels used in this study does not fix. Instead, for each PPG signal, the number of IMF channels is automatically adjusted based on the independence of IMF channels from each other using the covariance matrix¹². When the determinant of the matrix is above 0.8, the parameters are selected.

Stopping criteria parameters

$$\begin{cases} \epsilon_a = 5.10^{-6} \\ \epsilon_r = 5.10^{-3} \end{cases} \tag{5}$$

The IMFs which were decomposed from the raw PPG signal will be used to generate time-frequency spectrum by using Hilbert transform. This transform defines an analytic signal as:

$$z(t) = x(t) + i \cdot y(t) \tag{6}$$

$$y(t) = \frac{1}{\pi} P \int_{-\infty}^{+\infty} \frac{x(\tau)}{t - \tau} d\tau \tag{7}$$

Where x(t) is the IMF, y(t) is the Hilbert transform of x(t), P is the Cauchy principle. Then the time-frequency spectrum is:

$$H(f_0, t_0) = \sum_{i, f_i(t_0)}^N = f_0 a_i(t_0) \tag{8}$$

For each coordinate (t₀, f₀) in the spectrum, the spectrum value is the sum of all amplitudes of all IMFs at time t₀ with the respective frequency equal to f₀.

Where f, t are frequency and time point of interest, a(t) is the instantaneous amplitude at time, t, f(t) is the instantaneous frequency at time, t. The instantaneous amplitude and frequency of each IMF are calculate as follow:

The instantaneous amplitude

$$a(t) = \sqrt{x^2(t) + y^2(t)} \tag{9}$$

The instantaneous frequency

$$f(t) = \frac{1}{2\pi} \frac{d}{dt} \left[\arctan \frac{y(t)}{x(t)} \right] \tag{10}$$

Another advantage in implementing VMD and Hilbert transform is to filter out frequency band noise of signal without affect to the purity of original signal. This is conducted via chosen IMFs with central frequency regions ranging from 0.5Hz to 3Hz. The central frequency region is determined based on the mean and standard deviation of the instantaneous frequency of that IMF, specifically.

The average instantaneous frequency

$$\bar{f} = \frac{1}{T} \int_0^T f(t) dt \tag{11}$$

Standard deviation of the instantaneous frequency

$$\bar{s} = \sqrt{\frac{1}{T} \int_0^T (f(t) - \bar{f})^2 dt} \tag{12}$$

Then the central frequency range will be ($\bar{f} - \bar{s}, \bar{f} + \bar{s}$).

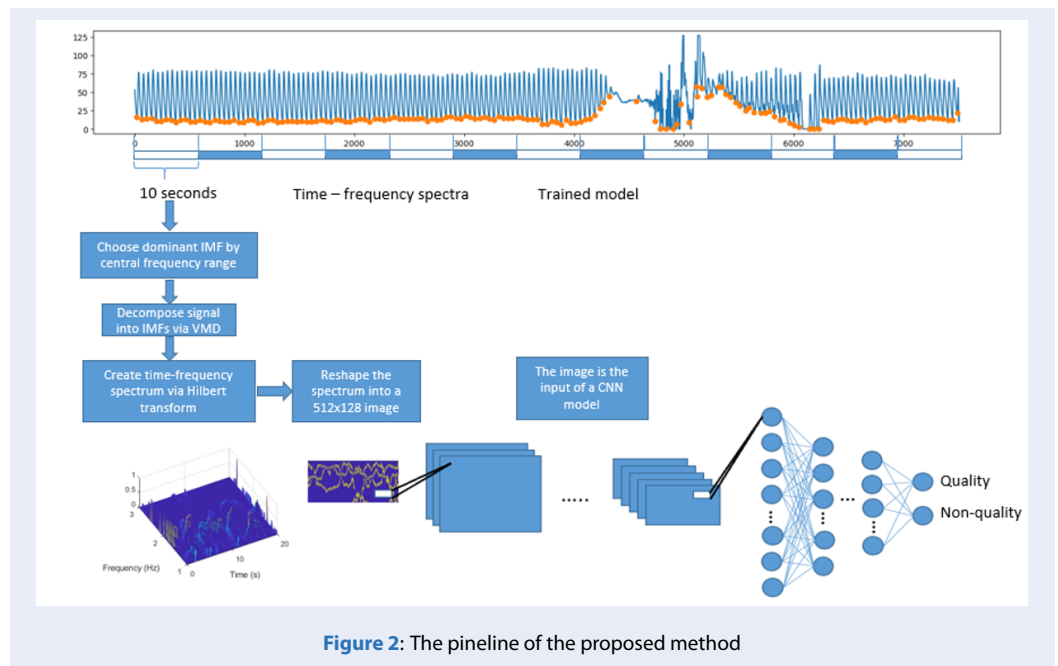


Figure 2: The pipeline of the proposed method

Proposed method

As mentioned earlier, the proposed methodology in this study relied on VMD and the Hilbert transform in conjunction with a CNN model. The pipeline illustrating the entire process is depicted in Figure 2.

Given the typical requirement of approximately 10 seconds of data length for most PPG signal applications, the raw PPG signal was segmented into 10-second segments with 1-second padding at both the start and end. Each segment underwent decomposition into Intrinsic Mode Functions (IMFs) using Variational Mode Decomposition (VMD). The mean and standard deviation of the instantaneous frequency of each IMF were computed to establish the central frequency range. An IMF exhibiting a central frequency range between 0.5Hz and 3Hz was selected as the dominant IMF. The dominant IMFs were utilized to construct a time-frequency spectrum via the Hilbert transform. Subsequently, the 1-second padding at the spectrum’s beginning and end was removed to mitigate the ‘end effect’ inherent in the Hilbert transform. The resulting spectrum was reshaped into a image. This image served as input for a CNN model designed to assess the quality of the PPG signal. The architecture of this model is detailed in Table 1. The entire method was implemented using the PyTorch framework and Python programming language.

Dataset

This study obtained PPG data from a cohort of subjects sourced from the open source MIMIC-III wave-

form database¹³. Each PPG signal in the dataset was segmented into 10-second segments with 1-second padding and labeled as either “good” or “not good” via the criteria from study of Elgendi et al.⁶. Figure 3 depicts the classify of PPG signal.

The training process utilized data from only 80% of the PPG segments in the MIMIC-III dataset. A detailed statistical description of the data is presented in Table 2.

METRIC

The model is evaluated based on its precision, accuracy, and recall, as most studies in this field have employed. The calculation formulas for these criteria are as follows:

Precision

$$Pre = \frac{TP}{TP + FP} \tag{13}$$

Recall

$$Re = \frac{TP}{TP + FN} \tag{14}$$

Accuracy

$$Acc = \frac{TP + TN}{FP + TP + TN + FN} \tag{15}$$

TP: The number of samples that are correctly classified as positive instances (i.e., the model predicts positive and the actual class is positive).

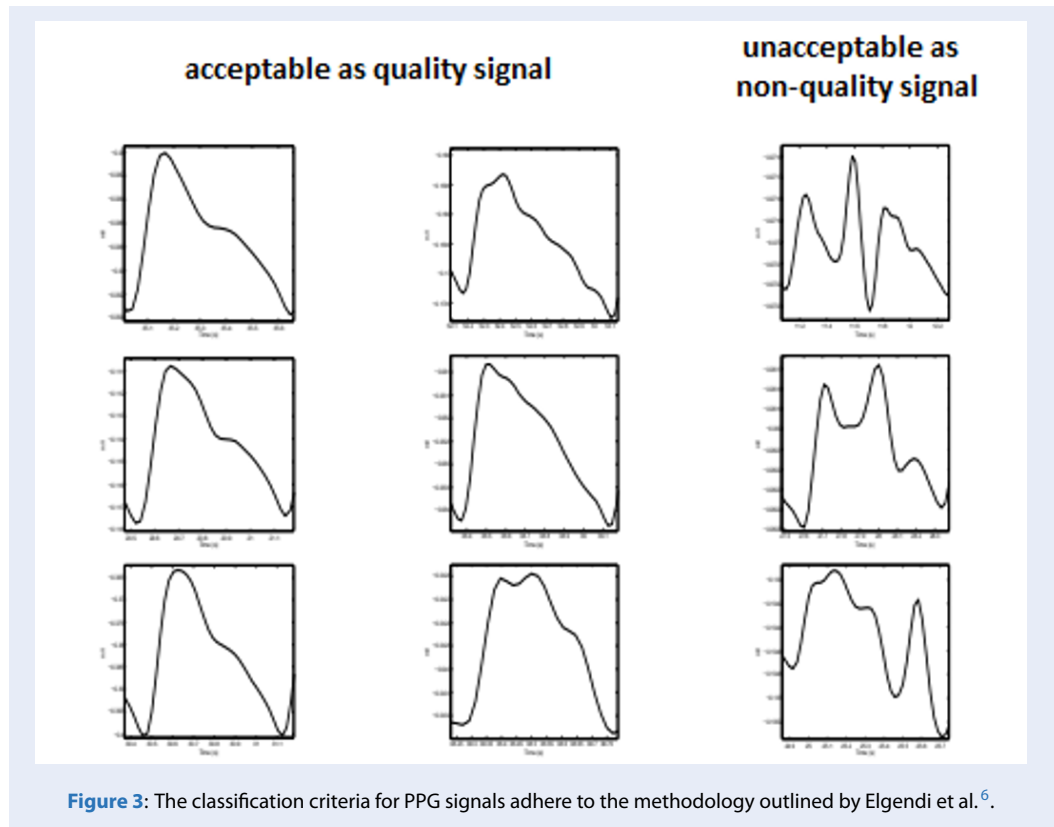
TN: The number of samples that are correctly classified as negative instances (i.e., the model predicts negative and the actual class is negative).

Table 1: Structure of the model

Layer	Type	Kernel	Strike	Channels	Shape
1	CNV	5×9	1	8	128×512×3
	LeakyReLU	-	-	-	128×512×8
	MAX	5×9	1	-	128×512×8
2	CNV	5×9	1	8	128×512×8
	LeakyReLU	-	-	-	128×512×8
	MAX	5×9	2	-	128×512×8
3	CNV	5×9	1	8	64×256×8
	LeakyReLU	-	-	-	64×256×16
	MAX	5×9	1	-	64×256×16
4	CNV	5×9	1	16	64×256×16
	LeakyReLU	-	-	-	64×256×16
	MAX	5×9	2	-	64×256×16
5	CNV	3×5	1	16	32×128×16
	LeakyReLU	-	-	-	32×128×16
	MAX	3×5	2	-	32×128×16
6	CNV	1×3	1	16	16×64×16
	LeakyReLU	-	-	-	16×64×16
	MAX	3×5	2	-	16×64×16
7	CNV	1×3	1	16	8×32×16
	LeakyReLU	-	-	-	8×32×16
	MAX	3×5	2	-	8×32×16
8	Fully connected layer	-	-	256	1024
9	Fully connected layer	-	-	-	256
10	Fully connected layer	-	-	-	150
11	Output	-	-	-	2

Table 2: Statistical description of the data.

MIMIC	140 subjects	
Total segment	3500 segments	
	Quality	Non - quality
Training set	912	1187
Validation set	316	383
Test set	354	346



FP: The number of samples that are incorrectly classified as positive instances (i.e., the model predicts positive but the actual class is negative).

FN: The number of samples that are incorrectly classified as negative instances (i.e., the model predicts negative but the actual class is positive).

RESULT

The training process consists of 45 epochs with a batch size of 512, learning rate of 0.0001. Figure 4 and Figure 5 illustrate the training and validation accuracy for each epoch. It is evident that the loss and accuracy values for both datasets are closely aligned, indicating the absence of overfitting.

The identification results for the test set demonstrate high performance. As shown in Table 3, the confusion matrix indicates an accuracy of 0.91, a precision of 0.95, and a recall of 0.88.

DISCUSSION

Compared to other time-frequency spectrum and deep model-based approaches, the proposed method achieves similar high performance with a simpler deep model. This advantage contributes to its implementation for applications on edge devices. Esgalhado et al. ⁸ utilized a hybrid CNN-LSTM model with



SSFT time-frequency spectrum input and achieved performance with accuracy 0.89, precision 0.92, and recall 0.91. In contrast, the proposed method only employed CNN and demonstrated comparable performance in terms of accuracy 0.91, precision 0.95, and recall 0.88. This disparity can be attributed to differences in time-frequency spectrum generation methods. Fourier-based methods, such as SSFT used in ⁸, exhibit energy leakage phenomena. This leads to less dense spectra, necessitating more complex models to enhance sparsity at each layer for accu-

Table 3: Confusion matrix of the proposed method’s result on test set.

Confusion matrix		True class	
		Positive	Negative
Predicated class	Positive	TP = 339	FP = 15
	Negative	FN = 44	TN = 302

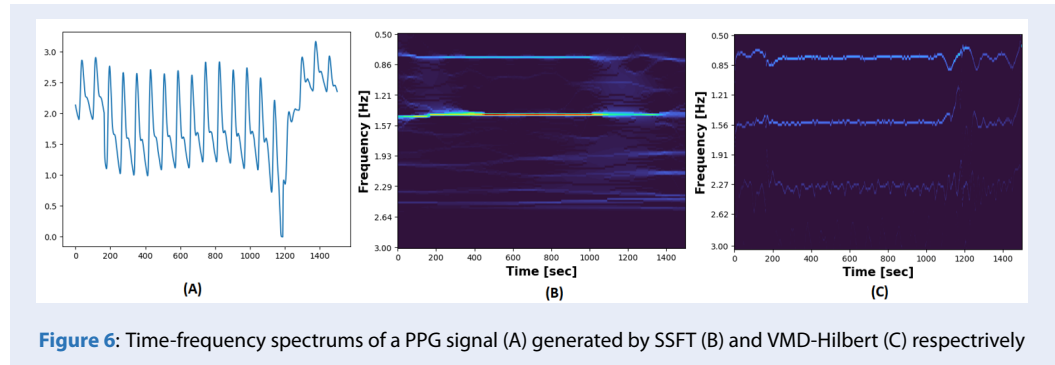


Figure 6: Time-frequency spectrums of a PPG signal (A) generated by SSFT (B) and VMD-Hilbert (C) respectively

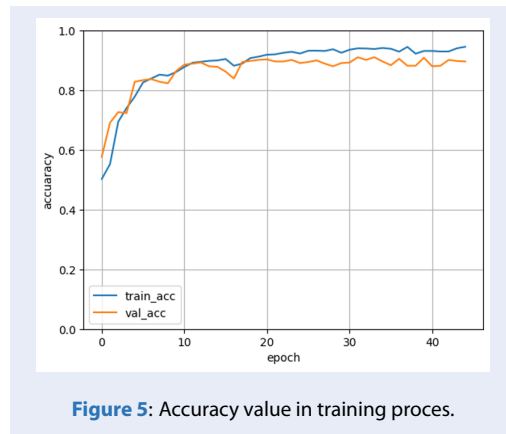


Figure 5: Accuracy value in training proces.

rate processing. Conversely, time-frequency spectra from VMD and Hilbert transform offer denser spectra, enabling simpler models to handle them more effectively. Figure 6 illustrates time-frequency spectra of the same PPG signal generated by SSFT and VMD-Hilbert methods, respectively. Upon initial inspection, the signal exhibits two disturbance segments around sample 200 and sample 1200, both of which are clearly depicted in both spectra with chaotic frequency zones at the respective samples. Moreover, there is a significant difference between the two spectra, influencing their effectiveness as model inputs. The spectrum generated by the VMD-Hilbert method features three distinct frequency modes around 0.84Hz, 1.56Hz, and 2.27Hz. In contrast, although also depicting two frequency modes around 0.84Hz and 1.56Hz, the spectrum from SSFT

exhibits significant energy leakage with numerous frequency zones, rendering the frequency mode at 2.27Hz nearly indistinct. The explanation for this disparity lies in the VMD method, which decomposes the signal into individual modes, each representing a specific frequency zone while preserving the signal’s non-linear and continuous instantaneous frequency characteristics. Due to its ability to separate frequency modes distinctly, it becomes easier to eliminate unrelated components, such as those induced by environmental noise, based on the central frequency range mentioned earlier. This process ensures that the final spectrum retains only the dominant frequency modes, revealing the essential aspects of the signal. In contrast, the SSFT analyzes the entire signal directly from the raw data. While the implementation of a bandpass filter can mitigate this issue, it risks eliminating crucial signal features, as noted in ¹⁴. Additionally, employing the Hilbert transform for each IMF enhances independence between individual IMFs. This independence contributes to the density of the spectrum compared to SSFT, which analyzes data along sliding windows without considering the independent nature of each frequency mode.

CONCLUSION

This paper presents a method for identifying and removing disturbed PPG segments. The algorithm’s key feature is based on the exceptional non-stationary analysis capabilities of VMD and the Hilbert transform. Despite the utilization of a deep model, it remains simple enough to be applied in practice with edge devices.

ACKNOWLEDGEMENTS

This research is funded by Department of Science and Technology under grant number 17/2023/HĐ-QKHCN. We acknowledge Ho Chi Minh City University of Technology (HCMUT), VNU-HCM for supporting this study.

LIST OF ABBREVIATIONS

PPG: Photoplethysmography
CNN: Convolutional neural network
CNV: Convolution layer
LSTM: Long short term memory
SSFT: Synchrosqueezed Fourier Transform
VMD: Variational Mode Decomposition
IMF: Intrinsic Mode Function
MAX: Max pooling layer

CONFLICTS OF INTERESTS

The authors declare no competing interests associated with the publication of this article.

AUTHORS' CONTRIBUTION

Thanh Trung Thai, Khanh Duy Phan: methodology,
Thanh Tung Luu: supervision, analysis.

REFERENCES

1. Allen J. Photoplethysmography and its application in clinical physiological measurement. *Physiol Meas.* 2007;28(3) ;PMID: 17322588. Available from: <https://doi.org/10.1088/0967-3334/28/3/R01>.
2. Elgendi M. On the analysis of fingertip photoplethysmogram signals. *Curr Cardiol Rev.* 2012;8:14-25;PMID: 22845812. Available from: <https://doi.org/10.2174/157340312801215782>.
3. Ram MR, Madhav KV, Krishna EH, Komalla NR, Reddy KA. A novel approach for motion artifact reduction in PPG signals based on AS-LMS adaptive filter. *IEEE Trans Instrum Meas.* 2012;61:1445-57; Available from: <https://doi.org/10.1109/TIM.2011.2175832>.
4. Selvaraj N, et al. Statistical approach for the detection of motion/noise artifacts in photoplethysmogram. In: 2011 Annual International Conference of the IEEE Engineering in Medicine and Biology Society; 2011; Boston, MA, USA. IEEE; 2011. p. 4972-5;PMID: 22255454. Available from: <https://doi.org/10.1109/IEMBS.2011.6091232>.
5. Hanyu S, Xiaohui C. Motion artifact detection and reduction in PPG signals based on statistics analysis. In: 2017 29th Chinese Control and Decision Conference (CCDC); 2017; Nanjing, China. IEEE; 2017; Available from: <https://doi.org/10.1109/CCDC.2017.7979043>.
6. Elgendi M. Optimal signal quality index for photoplethysmogram signals. *Bioengineering.* 2016;3(4):21;PMID: 28952584. Available from: <https://doi.org/10.3390/bioengineering3040021>.
7. Li Q, Clifford GD. Dynamic time warping and machine learning for signal quality assessment of pulsatile signals. *Physiol Meas.* 2012;33(9):1491;PMID: 22902950. Available from: <https://doi.org/10.1088/0967-3334/33/9/1491>.
8. Esgalhado F, Fernandes B, Vassilenko V, Batista A, Russo S. The application of deep learning algorithms for PPG signal processing and classification. *Computers.* 2021;10(12):158; Available from: <https://doi.org/10.3390/computers10120158>.
9. Zhang T, Fu C. Application of improved VMD-LSTM model in sports artificial intelligence. *Comput Intell Neurosci.* 2022;2022:1-9;PMID: 35875744. Available from: <https://doi.org/10.1155/2022/3410153>.
10. Huang NE, Shen Z, Long SR, Wu MC, Shih HH, Zheng Q, et al. The empirical mode decomposition and the Hilbert spectrum for nonlinear and non-stationary time series analysis. *Proc R Soc Lond A Math Phys Eng Sci.* 1998;454(1971):903-95; Available from: <https://doi.org/10.1098/rspa.1998.0193>.
11. Dragomiretskiy K, Zosso D. Variational mode decomposition. *IEEE Trans Signal Process.* 2013;62(3):531-44; Available from: <https://doi.org/10.1109/TSP.2013.2288675>.
12. Luu TT, et al. Amplitude percentage index study for beam vibration signal analysis based on EEMD. *J Eng Sci Technol.* 2022;17(6):3800-14.
13. Wang S, McDermott MB, Chauhan G, Ghassemi M, Hughes MC, Naumann T. Mimic-extract: A data extraction, preprocessing, and representation pipeline for MIMIC-III. In: *Proceedings of the ACM Conference on Health, Inference, and Learning*; 2020; Chicago, IL, USA. ACM; 2020. p. 222-35; Available from: <https://doi.org/10.1145/3368555.3384469>.
14. Cheng P, Chen Z, Li Q, Gong Q, Zhu J, Liang Y. Atrial fibrillation identification with PPG signals using a combination of time-frequency analysis and deep learning. *IEEE Access.* 2020;8:172692-706; Available from: <https://doi.org/10.1109/ACCESS.2020.3025374>.

Loại bỏ nhiễu tín hiệu PPG thông qua phân giải chế độ biến đổi và biến đổi Hilbert

Thái Thành Trung, Lưu Thanh Tùng*, Phan Khánh Duy

TÓM TẮT

Tín hiệu PPG cho thấy nhiều triển vọng như một kỹ thuật không xâm lấn trong các ứng dụng khác nhau. Tuy nhiên, để sử dụng hiệu quả tín hiệu này trong các tình huống thực tế, cần phải xử lý cẩn thận để nhận diện và khắc phục các nhiễu trong tín hiệu photo-plethysmography (PPG). Trong số các phương pháp đã được khám phá, việc tích hợp phổ thời gian-tần số với mô hình học sâu kết hợp, chẳng hạn như mô hình mạng nơ-ron tích chập – bộ nhớ dài ngắn hạn (CNN-LSTM), đã nổi lên như một phương pháp đầy hứa hẹn. Tuy nhiên, các phương pháp phổ biến thường dựa vào các thuật toán Fourier để trích xuất phổ thời gian-tần số, vốn dễ gặp vấn đề rò rỉ năng lượng. Để khắc phục hạn chế này, các phương pháp phân giải như Phân Giải Chế Độ Biến Đổi (VMD) kết hợp với biến đổi Hilbert cung cấp một giải pháp hấp dẫn. Trong nghiên cứu này, chúng tôi đề xuất một thuật toán mới sử dụng VMD và biến đổi Hilbert để trích xuất phổ thời gian-tần số làm đặc trưng cho mô hình mạng nơ-ron tích chập (CNN). Không giống như các nghiên cứu sử dụng phổ thời gian-tần số dựa trên Fourier và mô hình kết hợp CNN-LSTM, cách tiếp cận này áp dụng một kiến trúc đơn giản hơn, chỉ dựa vào mô hình CNN. Sự đơn giản này nhờ vào hiệu quả của VMD và biến đổi Hilbert trong việc trích xuất đặc trưng, giúp quá trình tính toán trở nên tinh gọn mà không giảm độ chính xác. Đáng chú ý, phương pháp của chúng tôi đạt được kết quả hiệu suất cao, với độ chính xác, độ chính xác và độ nhớ tương ứng là 0.91, 0.95, 0.88 trên bộ dữ liệu MIMICIII. Những kết quả này nhấn mạnh tính bền vững và hiệu quả của phương pháp đề xuất của chúng tôi, mở ra các hướng đi đầy hứa hẹn cho việc sử dụng tín hiệu PPG trong các ứng dụng y sinh học đa dạng. Bằng cách kết hợp các kỹ thuật xử lý tín hiệu tiên tiến với các mô hình học sâu, cách tiếp cận của chúng tôi góp phần vào sự tiến bộ của xử lý tín hiệu y sinh không xâm lấn, có tiềm năng trong giám sát và chẩn đoán sức khỏe.

Từ khóa: tín hiệu photo-plethysmography, xử lý tín hiệu photo-plethysmography

Bộ môn máy xây dựng và nâng chuyển,
Khoa Cơ khí, Trường Đại học Bách Khoa
– Đại học Quốc Gia TP.HCM, Việt Nam

Liên hệ

Lưu Thanh Tùng, Bộ môn máy xây dựng và
nâng chuyển, Khoa Cơ khí, Trường Đại học
Bách Khoa – Đại học Quốc Gia TP.HCM, Việt
Nam

Email: luuthanhtung2002@gmail.com

Lịch sử

- Ngày nhận: 03-3-2024
- Ngày chấp nhận: 04-7-2024
- Ngày đăng: 30-9-2024

DOI : <https://doi.org/10.32508/stdjet.v7i2.1346>



Bản quyền

© ĐHQG TP.HCM. Đây là bài báo công bố
mở được phát hành theo các điều khoản của
the Creative Commons Attribution 4.0
International license.



Trích dẫn bài báo này: Trung T T, Tùng L T, Duy P K. Loại bỏ nhiễu tín hiệu PPG thông qua phân giải chế độ biến đổi và biến đổi Hilbert. *Sci. Tech. Dev. J. - Eng. Tech.* 2024, 7(2):2258-2266.